Quantitative bone SPECT/CT applications for primary bone neoplasms

Kazuhiro Kitajima[1] MD, Hiroyuki Futani[2] MD, Hisashi Komoto[1] MD, Tatsuya Tsuchitani[3] BS, Yoshiyuki Takahashi[3] BS, Toshiya Tachibana[2] MD, Koichiro Yamakado[1] MD

1. Department of Radiology, Hyogo College of Medicine, Hyogo, Japan
2. Department of Orthopaedic Surgery, Hyogo College of Medicine, Hyogo, Japan
3. Department of Radiological Technology, Hyogo College of Medicine College Hospital, Hyogo, Japan

Keywords: Bone scintigraphy
- Primary bone neoplasm
- Quantitative SPECT/CT
- Standardized uptake value (SUV)

Corresponding author:
Kazuhiro Kitajima MD,
Department of Radiology, Hyogo College of Medicine,
Nishinomiya, Hyogo, Japan
1-1 Mukogawa-cho, Nishinomiya,
Hyogo 663-8501 Japan
Phone: +81-798-45-6883
Fax: +81-798-45-6262
kazu10041976@yahoo.co.jp

Received:
15 December 2020
Accepted revised:
24 March 2021

Abstract

Objective: To evaluate the clinical utility of quantitative values obtained with bone single photon emission computed tomography/computed tomography (SPECT/CT) for primary bone neoplasms. **Subjects and Methods:** Bone SPECT/CT scans of 23 patients with 19 benign bone neoplasms (5 osteoid osteomas, 4 bone giant cell tumor, 4 osteofibrous dysplasia, 3 intraosseous ganglion, 2 aneurysmal bone cyst, 1 intraosseous hemangioma) and 5 malignant bone neoplasms (2 osteosarcoma, 1 periosteal osteosarcoma, 1 malignancy in bone giant cell tumor, 1 Ewing sarcoma) were retrospectively analyzed with maximum standardized uptake value (SUVmax), peak SUV (SUVpeak), mean SUV (SUVmean), metabolic bone volume (MBV), and total bone uptake (TBU) of primary lesions. **Results:** Mean SUVmax of 19 benign and 5 malignant primary bone neoplasms were 6.89±3.26 (range 3.9-15.13) and 10.31±3.19 (5.0-13.45) respectively, with statistically significant difference (P=0.048). Mean SUVpeak of those were 5.87±2.83 (range 3.5-13.63) and 9.18±3.05 (4.09-12.03) respectively, with statistically significant difference (P=0.032). Mean SUVmean of those were 4.43±2.11 (range 2.59-9.37) and 7.13±2.90 (3.3-10.42) respectively, with statistically significant difference (P=0.027). Mean MBV of those were 22.0±30.0 (range 2.47-110.61) and 27.8±39.94 (8.59-99.24) respectively, with no statistically significant difference (P=0.72). Mean TBU of those were 80.64±94.57 (range 10.50-373.57) and 166.60±203.97 (28.68-528.13) respectively, with no statistically significant difference (P=0.17). **Conclusion:** Quantitative values obtained with bone SPECT/CT may serve as osteoblastic biomarkers for primary bone neoplasm.

Hell J Nucl Med 2021; 24(1): 36-44 *Epub ahead of print: 20 April 2021* *Published online: 30 April 2021*

Introduction

Although bone scintigraphy with technetium-99mmethyl diphosphonate (^{99m}Tc) MDPis widely used to evaluate osteoblastic activity of skeletal disease, it is technically difficult to quantify local tracer uptake using conventional bone scintigraphy, even with images acquired using single photon emission computed tomography (SPECT) [1, 2]. On the other hand, recent advances including integration of computed tomography (CT) for attenuation correction together with sophisticated reconstruction techniques have enabled quantitative measurements with SPECT/CT suitable for calculation of standardized uptake value (SUV) [3-5]. It is considered that quantitative SPECT/CT may soon have an enormous clinical effect in the practice of modern nuclear medicine by making imaging biomarkers available. Several recently published studies have demonstrated the clinical application of quantitative bone SPECT/CT for diagnosing bone metastasis [6, 7] and primary cartilaginous tumor [8]. However, to the best of our knowledge, no original studies of quantitative bone SPECT/CT for primary bone tumor have been presented and the clinical utility of quantitative bone SPECT/CT for diagnosing primary bone neoplasm has yet to be clarified.

The purpose of this study was to evaluate the characteristics of quantitative values obtained from bone SPECT/CT examinations of patients with primary bone tumors.

Subject and Methods

Patients

We searched all consecutive patients who visited Hyogo College of Medicine College Hospital on the suspicion of primary bone neoplasms between June 2018 and May 2020. Data from 109 patients with suspected primary bone neoplasm were reviewed retrospec-

tively. Patients who were evaluated with bone SPECT/CT scanning were included in this trial. Exclusion criteria were: not primary bone neoplasms for any reason and not have been evaluated with bone SPECT/CT examinations. Eighty-six patients were excluded from the study because 9 patients were found to have inflammatory bone disease, 10 patients were found to have metastatic bone disease and 67 patients with primary bone neoplasms were not evaluated with bone scintigraphy. Data of 23 patients (11 males, 12 females; mean age 36.9±22.1 years; range 7-74 years) were found to be eligible for our study. Our institutional review board granted approval for this retrospective review of clinical and imaging data and waived the need for obtaining informed consent from the patients. Among 23 patients, the final diagnosis was determined by the surgery or the biopsy (n=15) and findings of clinical and other radiological imaging modalities (n=8) such as X-ray, CT, or magnetic resonance imaging (MRI) (n=8). Patient and tumor characteristics are shown in Table 1. Five of the patients had osteoid osteoma of the ilium (n=1), femur (n=1), lumbar vertebra (n=1), fibula (n=1) or tibia (n=1). Four patients had bone giant cell tumor of the femur (n=2) or tibia (n=2). Three patients had osteofibrous dysplasia of the rib (n=3) or ulna (n=1). Three patients had intraosseous ganglion of the tibia (n=2) or femur (n=1). Two patients had aneurysmal bone cyst of the tibia (n=1) or ischium (n=1). One patient had intraosseous hemangioma of the femur. Whereas, two patients had high grade osteosarcoma of the femur, one patient had high grade periosteal osteosarcoma of the femur, one had malignancy in bone giant cell tumor of the femur and one had Ewing sarcoma of the fibula.

Bone scintigraphy

Three to 4 hours after intravenous administration of 555MBq ^{99m}Tc-hydroxymethylene diphosphonate (^{99m}Tc-HMDP), or adjusted for pediatric patients, as proposed by EANM [9]), planar bone scintigraphy was performed using a SPECT/CT scanner (NM/CT670; GE Healthcare, Pittsburgh, PA) equipped with a low-energy high-resolution collimator. A hybrid system was employed to acquire quantitative SPECT/CT images. The computed tomography images were initially obtained using the following parameters: tube voltage, 120kV; tube current, 40-80mA with "automA; GE Healthcare" function and noise level of 35; X-ray collimation, 20mm (16×1.25mm); table speed, 55mm/second; table feed, 27.5mm per rotation; tube rotation time, 0.5 seconds; pitch, 1.375:1; matrix, 512×512. CT images were reconstructed into 3.75mm thick sections with an adaptive statistical iterative reconstruction algorithm (ASiR; GE Healthcare). Next, single photon emission computed tomography images were acquired using an energy peak of 140.5KeV with a 7.5% window (130-151KeV), step-and-shot mode acquisition (15 seconds per step, 60 steps per detector) with a 3° angular increment, and a body contour scanning option. An extra window used for scatter correction was set at 120KeV with a 5% window (114-126KeV). For SPECT images, images were reconstructed with an iterative ordered subset expectation maximization algorithm (10 iterations, 10 subsets) using CT-based attenuation correction, scatter correction, and resolution recovery performed with software provided by the vendor (Volumetrix MI; GE Healthcare). A post-reconstruction filter was also applied (Gauss filter; frequency of 0.48, order of 10). Following reconstruction, images were set on a 128×128 matrix, with a 4.42-mm section thickness and 1.0 zoom factor.

Image analysis

The delineation of the volumes of interest (VOI) was performed by a board-certified nuclear medicine physician using a commercially available software GI-BONE (AZE Co., Ltd., Tokyo Japan), which reports the statistics for the various SUV, such as max (SUVmax), peak SUV (SUVpeak), mean (SUVmean), metabolic bone volume (MBV), and total bone uptake (TBU) [8]. SUVmax was defined as the maximum concentration in the target lesion (maximum radioactivity/voxel volume)/(injected radioactivity/body weight). Peak SUV is defined as average activity concentration within a 1cm^3 spherical VOI centered on the "hottest focus" within the tumor. As for SUVmean, that was calculated as summed SUV in each voxel in the target volume divided by the number of voxels within the target volume. MBL (mL) was measured automatically inside the tumor VOI, with the margin threshold set at 40% of SUVmax [10]. Total bone uptake (g) was expressed by the product of MBV and SUVmean.

Statistical analysis

The patients were divided into 2 groups, benign and malignant cartilaginous bone neoplasms. The mean value and SD for SUVmax, SUVpeak, SUVmean, MBV, and TBU were determined, with statistical differences assessed with t-test. All analysis was performed using the SAS software package, version 9.3 (SAS Institute, Cary, NC), and P values less than 0.05 were considered to indicate statistical significance.

Results

Maximum SUV, SUVpeak, SUVmean, MBV, and TBU for all 24 primary bone neoplasms with 19 benign and 5 malignant tumors are shown in Table 1. Six representative cases are shown in Figures 1-6.

Average SUVmax were 8.68±3.87 (range, 5.16-15.13) for osteoid osteoma (n=5), 6.86±4.26 (range, 3.90-13.19) for bone giant cell tumor (n=4), 7.71±2.45 (range, 4.46-9.72) for osteofibrous dysplasia (n=4), 5.42±2.09 (range, 3.01-6.70) for intraosseous ganglion (n=3), 4.09±1.65 (range, 2.66-5.52) for aneurysmal bone cyst (n=2), and 10.07±4.42 (range, 5.0-13.14) for high grade osteosarcoma (n=3) (Figure 7). Mean SUVmax of 19 benign and 5 malignant primary bone neoplasms were 6.89±3.26 (range 3.9-15.13) and 10.31±3.19 (5.0-13.45) respectively, with statistically significant difference (P=0.048).

Average SUVpeak were 7.63±3.47 (range, 4.98-13.63) for osteoid osteoma (n=5), 6.20±3.68 (range, 3.50-11.63) for bone giant cell tumor (n=4), 5.78±1.94(range, 3.53-7.93) for osteofibrous dysplasia (n=4), 4.80±1.95(range, 2.57-6.16) for intraosseous ganglion (n=3), 3.63±1.51(range, 2.32-4.94) for aneurysmal bone cyst (n=2) and 8.95±4.26 (range, 4.09-12.03)

Table 1. *Patient and tumor characteristics.*

Case	Sex	Age	Site	Diagnosis	SUVmax	SUVpeak	SUVmean	MBV	TBU
1	Female	34	ilium	osteoid osteoma	5.16	4.98	3.79	9.84	37.34
2	Male	13	tibia	osteoid osteoma	6.29	5.53	3.99	16.78	66.9
3	Female	43	lumbar vertebra	osteoid osteoma	8.64	6.88	4.91	6.12	30.1
4	Male	12	fibula	osteoid osteoma	8.19	7.11	5.21	4.72	24.58
5	Male	34	femur	osteoid osteoma	15.13	13.63	9.12	16.0	145.9
6	Female	37	tibia	bone giant cell tumor	3.9	3.5	2.59	92.95	241.1
7	Male	21	femur	bone giant cell tumor	5.14	4.7	3.71	45.13	167.3
8	Male	14	femur	bone giant cell tumor	5.22	4.95	3.38	110.61	373.6
9	Female	13	tibia	bone giant cell tumor	13.19	11.63	9.37	5.39	50
10	Female	46	ulna	Osteofibrous dysplasia	4.46	3.53	2.97	3.58	10.64
11	Male	54	rib	Osteofibrous dysplasia	7.18	4.92	4.26	2.47	10.5
			rib	Osteofibrous dysplasia	9.49	6.74	5.55	3.98	22.07
12	Male	67	rib	Osteofibrous dysplasia	9.72	7.93	6.87	3.32	22.78
13	Female	68	tibia	Intraosseous ganglion	3.01	2.57	1.83	11.14	20.35
14	Male	71	tibia	Intraosseous ganglion	6.54	5.67	3.79	16.67	63.09
15	Male	47	femur	Intraosseous ganglion	6.7	6.16	4.73	27.46	129.9
16	Female	47	tibia	Aneurysmal bone cyst	2.66	2.32	1.68	14.93	25.06
17	Female	20	ischium	Aneurysmal bone cyst	5.52	4.94	3.5	17.08	59.79
18	Female	74	femur	Intraosseous hemangioma	4.71	3.86	2.93	10.6	31.07
19	Female	63	femur	Osteosarcoma (high grade)	5	4.09	3.3	8.69	28.68
20	Female	7	femur	Osteosarcoma (high grade)	12.07	10.72	10.42	8.59	89.55
21	Female	10	femur	Osteosarcoma (high grade)	13.45	12.03	9.32	10.36	96.57
22	Male	39	femur	Malignancy in bone giant cell tumor	9.94	9.02	5.32	99.24	528.1
23	Male	14	fibula	Ewing sarcoma	11.38	10.05	7.31	12.32	90.09

SUV: standardized uptake value, MBV: metabolic bone volume, TBU: total bone uptake

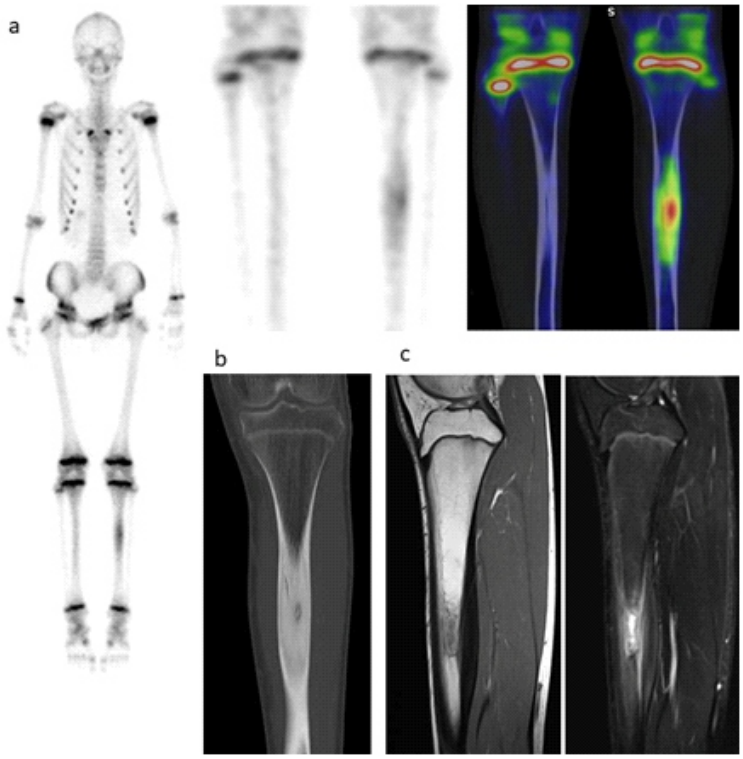

Figure 1. A 13-year-old male with osteoid osteoma (Case 2) of the left tibia underwent quantitative bone SPECT/CT scanning. Histological diagnosis of the biopsy was osteoid osteoma. a) Planar and SPECT/CT bone scintigraphy showing focal moderate radiotracer uptake at the diaphysis of the left tibia with SUVmax, SUVpeak, SUVmean, MBV and TBU values of 6.29, 5.53, 3.99, 16.78mL, and 66.9g, respectively. b) Coronal CT (bone windowing) showing cortical thickening with intense calcification and osteoblastic mass, called a "nidus", surrounded by a distinct zone of reactive bone sclerosis in the diaphysis of the left tibia. c) Coronal T1-weigthed MR image showing hypointense area and STIR image showing intense hyperintense area, corresponding to nidus at the diaphysis of the left tibia.

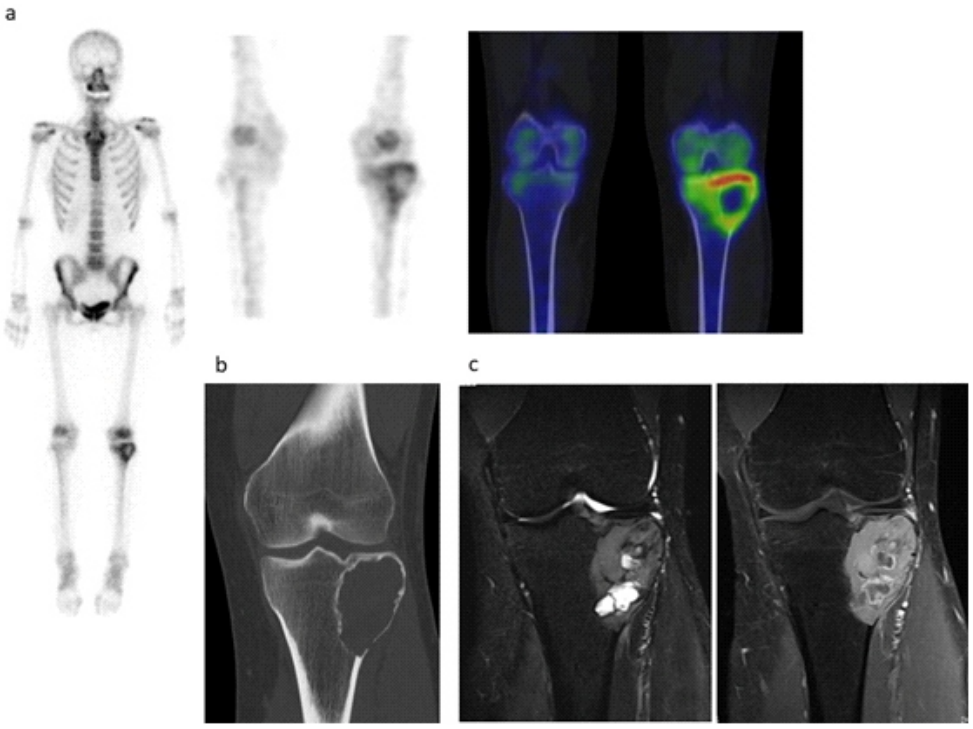

Figure 2. A 37-year-old female with bone giant cell tumor (Case 6) of the left tibia underwent preoperative quantitative bone SPECT/CT scanning. Histological diagnosis of the surgical specimen was bone giant cell tumor. a) Planar and SPECT/CT bone scintigraphy showing peripherally focal moderate radiotracer uptake at the proximal epiphysis of the left tibia with SUVmax, SUVpeak, SUVmean, MBV and TBU values of 3.9, 3.5, 2.59, 92.95mL, and 241.1g respectively. b) Coronal CT (bone windowing) showing an oval epiphyso-metaphyseal pure lytic lesion at the proximal epiphysis of the left tibia. c) Coronal STIR image showing hyperintense mass with intense hyperintense cystic component and Gd-enhanced fat-suppressed image showing strong enhancement of the solid component at the proximal epiphysis of the left tibia.

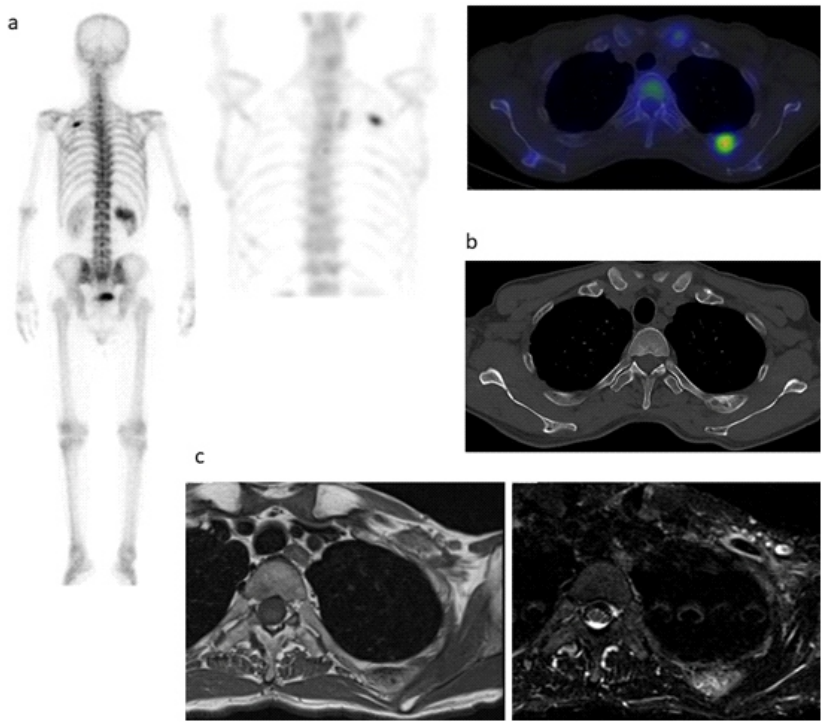

Figure 3. A 67-year-old male with osteofibrous dysplasia (Case 12) of the left rib underwent quantitative bone SPECT/CT scanning. a) Planar and SPECT/CT bone scintigraphy showing peripherally focal intense radiotracer uptake at the left rib with SUVmax, SUVpeak, SUVmean, MBV and TBU values of 9.72, 7.93, 6.87, 3.32mL, and 22.78g, respectively. b) Axial CT (bone windowing) showing an expansive lytic lesion combined with osteosclerosis at the left rib. c) Axial T1WI image showing heterogeneous hypointense area with intense hyperintense cystic component and STIR image showing heterogeneous hyperintense area at the left rib.

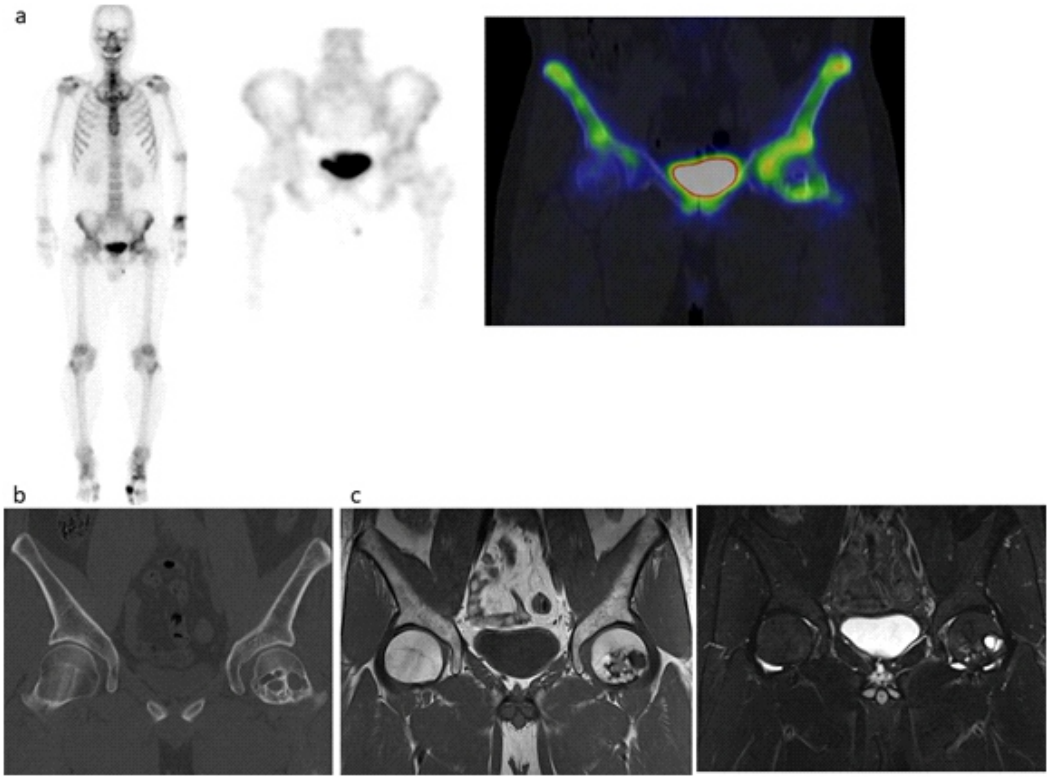

Figure 4. A 47-year-old male with intraosseous ganglion (Case 15) of the left femur underwent preoperative quantitative bone SPECT/CT scanning. Histological diagnosis of the surgical specimen was intraosseous ganglion. a) Planar and SPECT/CT bone scintigraphy showing peripherally focal moderate radiotracer uptake at the proximal epiphysis of the left femur with SUVmax, SUVpeak, SUVmean, MBV and TBU values of 6.70, 6.16, 4.73, 27.46mL, and 129.9g respectively. b) Coronal CT (bone windowing) showing an oval multilocular and pure lytic lesion at the proximal epiphysis of the left femur. c) Coronal T1WI image showing multilocular hypointense mass and STIR image showing hyperintense mass at the proximal epiphysis of the left tibia.

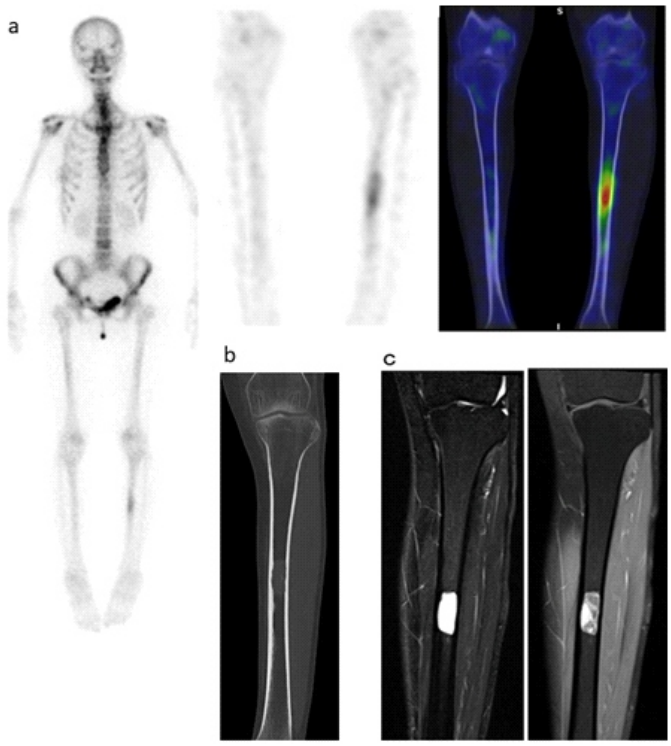

Figure 5. A 47-year-old female with aneurysmal bone cyst (Case 16) of the left tibia underwent preoperative quantitative bone SPECT/CT scanning. Histological diagnosis of the surgical specimen was aneurysmal bone cyst. a) Planar and SPECT/CT bone scintigraphy showing focal mild radiotracer uptake at the diaphysis of the left tibia with SUVmax, SUVpeak, SUVmean, MBV and TBU values of 3.9, 3.5, 2.59, 92.95mL, and 241.1g, respectively. b) Coronal CT (bone windowing) showing an oval osteolytic lesion at the diaphysis of the left tibia. c) Coronal STIR image showing hyperintense mass with intense hyperintense cystic component and Gd-enhanced fat-suppressed T1WI image showing heterogeneous enhancement of the mass at the diaphysis of the left tibia.

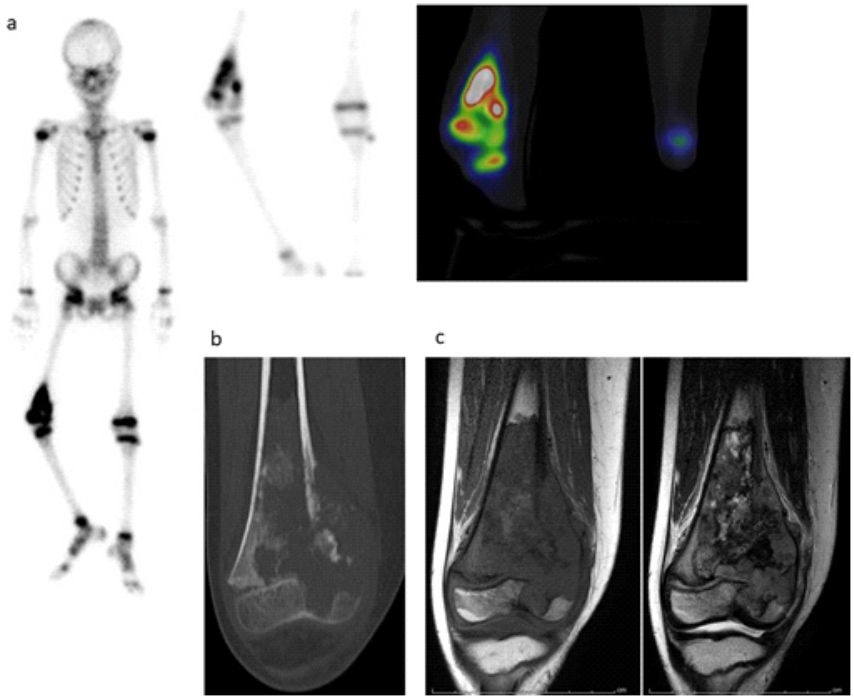

Figure 6. A 7-year-old female with osteosarcoma (Case 20) of the right femur underwent preoperative quantitative bone SPECT/CT scanning. Histological diagnosis of the surgical specimen after the neoadjuvant chemotherapy was osteosarcoma. a) Planar and SPECT/CT bone scintigraphy showing focal heterogeneous intense radiotracer uptake at the distal epiphysis and metaphysis of the right femur with SUVmax, SUVpeak, SUVmean, MBV and TBU values of 12.07, 10.72, 10.42, 8.59mL, and 89.55g respectively. b) Coronal CT (bone windowing) showing destructive mass with periosteal reaction at the proximal epiphysis of the right femur. c) Coronal T1WI image showing heterogeneous hypointense mass invading bone marrow and cortex and T2WI image showing heterogeneous hypointense and hyperintense mixed mass at distal epiphysis and metaphysis of the right femur.

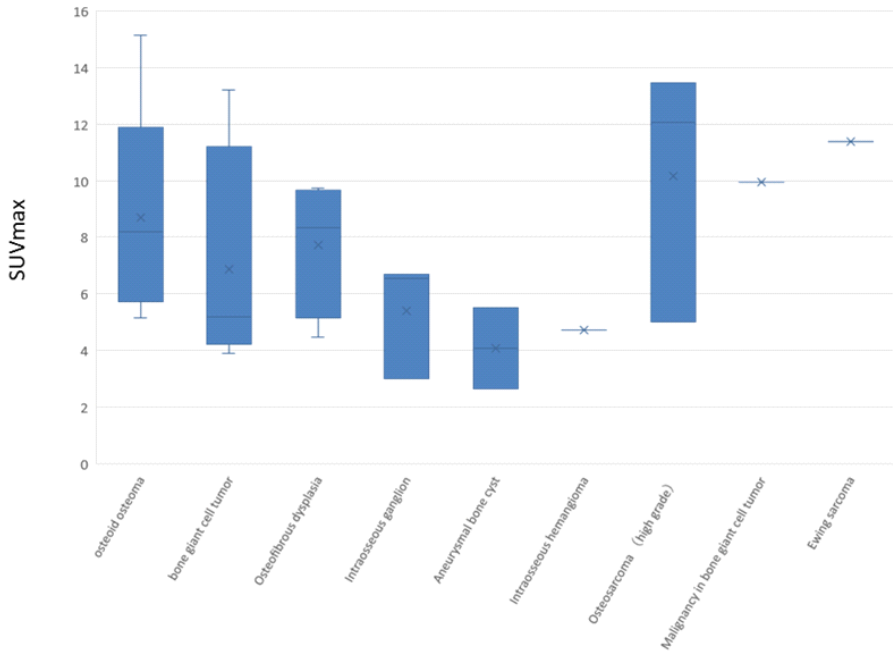

Figure 7. Box-Whiskerplots SUVmax for every primary bone tumor.

for high grade osteosarcoma (n=3). Mean SUVpeak of 19 benign and 5 malignant primary bone neoplasms were 5.87± 2.83 (range 3.5-13.63) and 9.18±3.05 (4.09-12.03) respectively, with statistically significant difference (P=0.032).

Average SUVmean were 5.40±2.16 (range, 3.79-9.12) for osteoid osteoma (n=5), 4.76±3.11(range, 2.59-9.37) for bone giant cell tumor (n=4), 4.91±1.68 (range, 2.97-6.87) for osteofibrous dysplasia (n=4), 3.45±1.48 (range, 1.83-4.73) for intraosseous ganglion (n=3), 2.59±1.05 (range, 1.68-3.50) for aneurysmal bone cyst (n=2) and 7.68±3.83 (range, 3.3-10.42) for high grade osteosarcoma (n=3). Mean SUVmean of 19 benign and 5 malignant primary bone neoplasms were 4.43±2.11 (range 2.59-9.37) and 7.13±2.90 (3.3-10.42) respectively, with statistically significant difference (P=0.027).

Average MBV were 10.69±5.54 (range, 4.72-16.78) for osteoid osteoma (n=5), 63.52±47.61 (range, 5.39-110.61) for bone giant cell tumor (n=4), 3.34±0.64 (range, 2.47-3.98) for osteofibrous dysplasia (n=4),18.42±8.30 (range, 11.14-27.46) for intraosseous ganglion (n=3), 16.01±1.24 (range, 14.93-17.08) for aneurysmal bone cyst (n=2) and 9.21±0.99(range, 8.59-10.36) for high grade osteosarcoma (n=3). Mean MBV of 19 benign and 5 malignant primary bone neoplasms were 22.0±30.0 (range 2.47-110.61) and 27.8±39.94 (8.59-99.24) respectively, with no statistically significant difference (P= 0.72).

Average TBU were 60.97±50.23 (range, 24.58-145.94) for osteoid osteoma (n=5), 207.98±135.56 (range, 50.0-373.57) for bone giant cell tumor (n=4), 16.50±6.85 (range, 10.50-22.78) for osteofibrous dysplasia (n=4), 71.13±55.24 (range, 20.35-129.94) for intraosseous ganglion (n=3), 42.43±20.05 (range, 25.06-59.79) for aneurysmal bone cyst (n=2), and 71.60±37.34(range, 28.68-96.57) for high grade osteosarcoma (n=3). Mean TBU of 19 benign and 5 malignant primary bone neoplasms were 80.63±94.57 (range 10.50-373.57) and 166.60±203.97 (28.68-528.13) respectively, with no statistically significant difference (P=0.17).

Discussion

This is the first original paper to present findings showing effective clinical application of quantitative bone SPECT/CT for primary bone neoplasms. Although we found that SUVmax, SUVpeak, and SUVmean of primary malignant bone neoplasms were statistically significantly higher than those of primary benign bone neoplasms, there was considerable overlap between primary malignant and benign bone neoplasms and therefore SUVmax, SUVpeak, and SUVmean may not be useful to differentiating malignant from benign primary bone neoplasms in clinical situation. Although we have already reported cases of periosteal osteosarcoma and Paget disease in case reports [10,11], we suggest that quantitative bone SPECT/CT can be useful to evaluate treatment response of primary bone disease. In the past, scintigraphy without quantitative values used to show subjective and ambiguous evaluation of the efficacy of treatment response in affected patients. However, quantitative SPECT/CT with SUV and volume can produce objective and persuasive evaluation of the efficacy of treatment response in affected patients. Quantitative SPECT/CT is noninvasive and we hope its use to increase the monitoring accuracy in the of treatment response evaluation.

Single photon emission tomography/CT is a state-of-the-art modality that produces objective quantitative data and it is known to be a powerful investigative tool in clinical practice. Using results of robust algorithms for CT-based attenuation correction, scatter correction and resolution re-

covery, SPECT/CT generates imaging voxels, denoted as units of radioactivity per volume [i.e., kilobecquerels (kBq)/mL]. This is a fundamental difference compared to traditional nuclear medicine imaging methods, such as planar scintigraphy, SPECT and non-quantitative SPECT/CT, with which counts per second are used to produce imaging units. With quantitative SPECT/CT, lesion radioactivity can be normalized to radioactivity activity, resulting in quantitative parameter values, such as percent injected dose and SUV [3-5]. Zeintl et al. (2010) [3] found that advanced SPECT/CT technology can facilitate quantitative ^{99m}Tc SPECT imaging with excellent accuracy in both phantom (error <3.6%) and patient (error <1.1%) studies. Furthermore, in a phantom study, Gnesin et al. (2016) [5] reported that both absolute and concentration activity results determined with quantitative ^{99m}Tc SPECT/CT were within 10% of the expected values.

Osteoid osteoma is a type of benign bone-forming tumor, which accounts for 10%-12% of all benign bone tumors. Osteoid osteoma has unique and quite often diagnostic symptoms; the typical clinical symptom is long term pain of increasing severity. It is characterized by a well-demarcated osteoblastic mass, called a "nidus", surrounded by a distinct zone of reactive bone sclerosis [12]. It was reported that >50% of osteoid osteomas occur in the long bones of the lower extremities; in addition, they are often present in the small bones of the hand and foot. Technetium-99-bone scintigraphy generally shows non-specific increased uptake in almost all osteoid osteoma lesions.

Bone giant cell tumor is typically a rare benign tumor (about 5%-10% of bone primary tumors), and usually, it appears as an osteolytic epiphyseal long bone tumor. Bone giant cell tumor affects primarily young adults, has aggressive character and possibility of malignant transformation. It has mostly histological diagnosis and it specially affects epiphyso-metaphyseal regions of long bones of members. Typically, it is an oval or rounded epiphyso-metaphyseal pure lytic lesion, standard geographical lacuna, sometimes limited by condensed edging [13]. Bone scintigraphy shows increased uptake in the vastest majority of bone giant cell tumor. Increased uptake peripherally with central photopenia (doughnut sign) was seen in 57% of cases [14].

Osteofibrous dysplasia is typically benign, self-limiting condition that usually occurs in the first two decades of life, accounting for about 0.2% of all primary bone tumors. Microscopically, osteofibrous dysplasia has a fibrous stroma with spicules of woven bone surrounded by osteoblasts with distinct zonal architecture. It is typically located in the mid-tibia and present as expansile lytic lesions with variable degrees of osteolysis and osteosclerosis [15]. Lysis may present as a single focus, multiple "bubble-like" or elongated linear foci interspersed with reactive bone. Technetium-99-bone scintigraphy generally shows non-specific increased uptake in almost all fibro-osseous lesions.

Aneurysmal bone cyst is rapidly growing benign bone tumors that account for 1%-2% of all primary bone tumors. Aneurysmal bone cyst is a benign, expansile osteolytic lesion containing thin-walled, blood-filled cystic cavities. It commonly involves the metaphysis of long tubular bones, vertebrae or flat bones of patients younger than 20 years [16]. Bone scintigraphy shows increased uptake throughout the lesion or predominantly in the periphery[17].

Osteosarcoma is a tumor characterized by the malignant proliferation of osteoid-producing mesenchymal spindle cells and is the most common primary bone malignancy in children and adolescents [18]. Ewing sarcoma (a member of the Ewing sarcoma family of tumors) is the second most common malignant bone tumor in pediatrics. Ewing sarcoma is considered a small round blue cell tumor, thought to originate in neural crest cells. Technetium-99-bone scintigraphy generallyshows non-specific increased uptake in almost all osteosarcoma and Ewing sarcoma lesions, and is also useful detecting osseous metastatic lesions.

The main limitations of this study are the small subject population and lack of histological confirmation for all benign disease. However, it would have been unethical to investigate all affected patients using invasive procedures. We consider that diagnosis of primary benign skeletal disease based on radiological imaging and follow-up results is clinically valid. Nevertheless, the usefulness of quantitative values obtained with bone SPECT/CT in patients with primary bone tumor should be tested with a larger cohort.

In conclusion, quantitative values obtained with bone SPECT/CT may serve as osteoblastic biomarkers for primary bone neoplasm. In the future, we need to evaluate the usefulness of quantitative bone SPECT/CT for evaluating treatment response of primary bone neoplasm to determine whether quantitative bone SPECT/CT has the potential to improve the management of primary skeletal disease.

Acknowledgement
This work was supported by JSPS KAKENHI grant numbers 19K08187.

The authors declare that they have no conflicts of interest.

Bibliography

1. Pietrzak A, Czepczynski R, Wierzchoslawska E, Cholewinski W. Metabolic activity in bone metastases of breast and prostate cancer were similar as studied by 18F-FDG PET/CT. The role of ^{99m}Tc-MDP. *Hell J Nucl Med* 2017; 20: 237-40.
2. Mavriopoulou E, Zampakis P, Smpiliri E et al. Whole body bone SPET/CT can successfully replace the conventional bone scan in breast cancer patients. A prospective study of 257 patients. *Hell J Nucl Med* 2018; 21: 125-33.
3. Zeintl J, Vija AH, Yahil A et al. Quantitative accuracy of clinical ^{99m}Tc SPECT/CT using ordered-subset expectation maximization with 3-dimensional resolution recovery, attenuation, and scatter correction. *J Nucl Med* 2010; 51: 921-8.
4. Bailey DL, Willowson KP. An evidence-based review of quantitative SPECT imaging and potential clinical applications. *J Nucl Med* 2013; 54: 83-9.
5. Gnesin S, Leite Ferreira P, Malterre J et al. Phantom validation of Tc-99m absolute quantification in a SPECT/CT commercial device. *Comput Math Methods Med* 2016; 2016: 4360371.
6. Kuji I, Yamane T, Seto Aet al. Skel et al standardized uptake values obtained by quantitative SPECT/CT as an osteoblastic biomarker for the discrimination of active bone metastasis in prostate cancer. *Eur J Hybrid Imaging* 2017; 1: 2.
7. Tabotta F, Jreige M, Schaefer N et al. Quantitative bone SPECT/CT: high specificity for identification of prostate cancer bone metastases. B*MC Musculoskelet Disord* 2019; 20: 619.
8. Kitajima K, Futani H, Tsuchitani T et al. Quantitative bone SPECT/CT applications for cartilaginous bone neoplasms. *Hell J Nucl Med* 2020; 23: 133-7.

9. Lassmann M, Biassoni L, Monsieurs M et al. EANM Dosimetry and Paediatrics Committees. The new EANM paediatric dosage card. *Eur J Nucl Med Mol Imaging* 2007; 34: 796-8.
10. Kitajima K, Futani H, Fujiwara M et al. Usefulness of quantitative bone single photon emission computed tomography/computed tomography for evaluating response to neoadjuvant chemotherapy in a patient with periosteal osteosarcoma. *Cureus* 2018; 10: e3655.
11. Kitajima K, Futani H, Tsuchitani T et al. Quantitative bone single photon emission computed tomography/computed tomography for evaluating response to bisphosphonate treatment in patients with Paget's disease of bone. *Case Rep Oncol* 2020; 13: 829-34.
12. Park JH, Pahk K, Kim Set al. Radionuclide imaging in the diagnosis of osteoid osteoma. *Oncol Lett* 2015; 10: 1131-4.
13. Oueriagli SN, Ghfir I, Guerrouj HE, Raïs NB. What role for radiobiphosphonates bone scintigraphy in the monitoring of an unusual bone giant cell tumor: a case report and literature review. *Am J Nucl Med Mol Imaging* 2016; 6: 128-34.
14. Levine E, DeSmet AA, Neff JR, Martin NL. Scintigraphic evaluation of giant cell tumor of bone. *Am J Roentgenol* 1984; 148: 343-8.
15. Bethapudi S, Ritchie DA, Macduff E, Straiton J. Imaging in osteofibrous dysplasia, osteofibrous dysplasia-like adamantinoma, and classic adamantinoma. *Clin Radiol* 2014; 69: 200-8.
16. Hermann AL, Polivka M, Loit MP et al. Aneurysmal bone cyst of the frontal bone - A radiologic-pathologic correlation. *J Radiol Case Rep* 2018; 12: 16-24.
17. Song W, Suurmeijer AJH, Bollen SM et al. Soft tissue aneurysmal bone cyst: six new cases with imaging details, molecular pathology, and review of the literature. *Skeletal Radiol* 2019; 48: 1059-67.
18. Kaste SC. Imaging pediatric bone sarcomas. *Radiol Clin North Am* 2011; 49:749-65.